Quaternary Science Reviews 82 (2013) 13–22

Contents lists available at ScienceDirect

Quaternary Science Reviews

journal homepage: www.elsevier.com/locate/quascirev

Rapid ice retreat in Disko Bugt supported by ^{10}Be dating of the last recession of the western Greenland Ice Sheet

Samuel E. Kelley [a,*], Jason P. Briner [a], Nicolás E. Young [b]

[a] Department of Geology, University at Buffalo, Cooke 411, Buffalo, NY 14260, USA
[b] Lamont-Doherty Earth Observatory, Comer 217, P.O. Box 1000, Palisades, NY 10904, USA

ARTICLE INFO

Article history:
Received 28 May 2013
Received in revised form
20 September 2013
Accepted 23 September 2013
Available online 26 October 2013

Keywords:
Greenland Ice Sheet
Disko Bugt
^{10}Be dating
Ice dynamics
Retreat rates

ABSTRACT

Due to rising sea levels and warming ocean currents, marine-based sectors of the Greenland and Antarctic ice sheets are particularly vulnerable to warming climate. Reconstructions of the timing of marine-based ice margin fluctuations in Greenland during the early Holocene can provide context for historical and modern observations of ice-sheet change. Here, we generate a ^{10}Be chronology of ice-sheet retreat through Disko Bugt, western Greenland. Our new chronology, consisting of twelve ^{10}Be ages from sites surrounding and within Disko Bugt, fills a gap in the history of the western margin of the Greenland Ice Sheet and allows for a continuous composite record of ice-margin recession between the continental shelf break and the current margin. We constrain the onset of ice-margin retreat from outer Disko Bugt to 10.8 ± 0.5 ka. When combined with previous chronologies, these results place the final Greenland Ice Sheet retreat out of Disko Bugt onto land at Jakobshavn Isfjord and Qasigiaanguit at 10.1 ± 0.3 ka, and later at 9.2 ± 0.1 ka in southeastern Disko Bugt. The rate of retreat during this time period is between ~50–450 m a^{-1} for central Disko Bugt and ~50–70 m a^{-1} along the southern coast of Disko Bugt. Deglaciation of Disko Bugt occurred ~1000 years later than in neighboring Uummannaq Fjord to the north. This asynchrony in the timing of deglaciation suggests that local ice dynamics played an important role in the retreat of the Greenland Ice Sheet from large marine embayments in western Greenland.

1. Introduction

Interest in the Greenland Ice Sheet (GrIS) has grown in recent years as investigations have demonstrated drastic Arctic warming during the 20th century, including ~2 °C in western Greenland (Box, 2002; Kaufman et al., 2009; Fisher et al., 2012; Perren et al., 2012). Warming in the Arctic has been shown to outpace global temperature rise, with the warming intensified through positive feedbacks, such as those related to Arctic Ocean sea-ice cover (Serreze et al., 2009; Miller et al., 2010; Maslanik et al., 2011). This accelerated warming is important for future sea-level rise predictions, as the increase in mass lost from Earth's ice sheets, such as the GrIS, is expected to become the dominant factor in eustatic sea-level rise, soon surpassing contributions to sea-level rise from ice caps and alpine glaciers and thermal expansion of the oceans (Meier et al., 2007; Joughin et al., 2010; Rignot et al., 2011).

Records of past glacier fluctuations spanning the Holocene are necessary to place firsthand ice-margin observations from historic accounts, aerial photographs, and satellite imagery in the broader context of pre-historic ice margin fluctuations (e.g. Weidick, 1968; Weidick, 1994; Rignot and Kanagaratnam, 2006; Csatho et al., 2008; Bjørk et al., 2012; Kjær et al., 2012). Recent efforts have led to increasingly robust terrestrial chronologies for GrIS margin fluctuations during the Holocene (e.g. Weidick et al., 1990; Kaplan et al., 2002; Weidick et al., 2004; Möller et al., 2010; Hughes et al., 2012; Kelley et al., 2012; Levy et al., 2012; Roberts et al., 2013; Young et al., 2013a). Reconstructions of ice-margin fluctuations from land have revealed the timing of multiple local re-advances or standstills throughout the Holocene (e.g. Kelley et al., 2012; Levy et al., 2012; Young et al., 2013a). Studies of the latest Pleistocene and earliest Holocene recession of the GrIS from the western continental shelf reveal asynchronous retreat of ice streams that crossed the continental shelf (e.g. McCarthy, 2011; Ó Cofaigh et al., 2013).

Despite ice margin reconstructions at specific locations or for specific time periods, complete records tracking the ice margin position from the Last Glacial Maximum position to the present are lacking in Greenland. Here, we present a cosmogenic ^{10}Be exposure dating (hereafter ^{10}Be dating) chronology of ice retreat through Disko Bugt, bridging previously published ice margin chronologies

* Corresponding author.
E-mail address: samuelke@buffalo.edu (S.E. Kelley).

0277-3791/$ – see front matter © 2013 Elsevier Ltd. All rights reserved.
http://dx.doi.org/10.1016/j.quascirev.2013.09.018

from the continental shelf and from farther inland in the Disko Bugt region (Weidick et al., 1990; Briner et al., 2010; McCarthy, 2011; Ó Cofaigh et al., 2013; Young et al., 2013a). This record affords a view into past changes in the position of the GrIS in Disko Bugt throughout the Holocene and gives insight into how an ice sheet recedes through large marine embayments.

2. Disko Bugt

Disko Bugt is a large marine embayment situated on the central-west Greenland coast bordered by Baffin Bay to the west and as wide as 50-km-widea strip of ice-free land fringing the GrIS to its east (Fig. 1). At present, Disko Bugt receives ice discharge from Jakobshavn Isbræ, an outlet glacier responsible for ~7% of mass loss and ~10% of iceberg discharge from the GrIS (Bindschadler, 1984; Weidick and Bennike, 2007), as well as from five other marine outlet glaciers. Water depths in Disko Bugt average 200–400 m, with a pronounced southwest–northeast-oriented trough crossing the center of the bay where water depths exceed 600 m. Additionally, a bedrock controlled bathymetric high, expressed subaerially as small island groups, spans the western margin of Disko Bugt. The bathymetric high is bisected south of the island of Nunarssuaq by a trough oriented southwest–northeast (Fig. 1). Numerous E–W streamlined bedforms on the floor of Disko Bugt suggest fast flowing ice through Disko Bugt in the past (Ó Cofaigh et al., 2013). This pattern is also expressed on land where glacially-streamlined landscapes suggest the presence of a former ice stream (Roberts and Long, 2005). The landscape south and east of Disko Bugt consists of glacially sculpted Precambrian crystalline bedrock and landforms indicative of extensive glacial erosion (Chalmers et al., 1999; Roberts and Long, 2005). Disko Island forms the northern boundary of Disko Bugt, and is composed of primarily Cretaceous-Tertiary clastic-sediments overlain by Tertiary flood basalts and small outcrops of Precambrian crystalline bedrock (Chalmers et al., 1999).

Funder and Hansen (1996) proposed a two-stage model of deglaciation for the GrIS depicting rapid initial deglaciation from the continental shelf due to rising eustatic sea level, driving the eastward retreat of the GrIS margin to the coast by 10 ka. Following retreat to the coast, eastward movement slowed and was driven primarily by surface ablation. Recent work has refined the timing of deglaciation and subsequent re-advances, though the Funder and Hansen (1996) conceptual model remains largely unmodified. Marine cores from the continental shelf west of Disko Bugt give rise

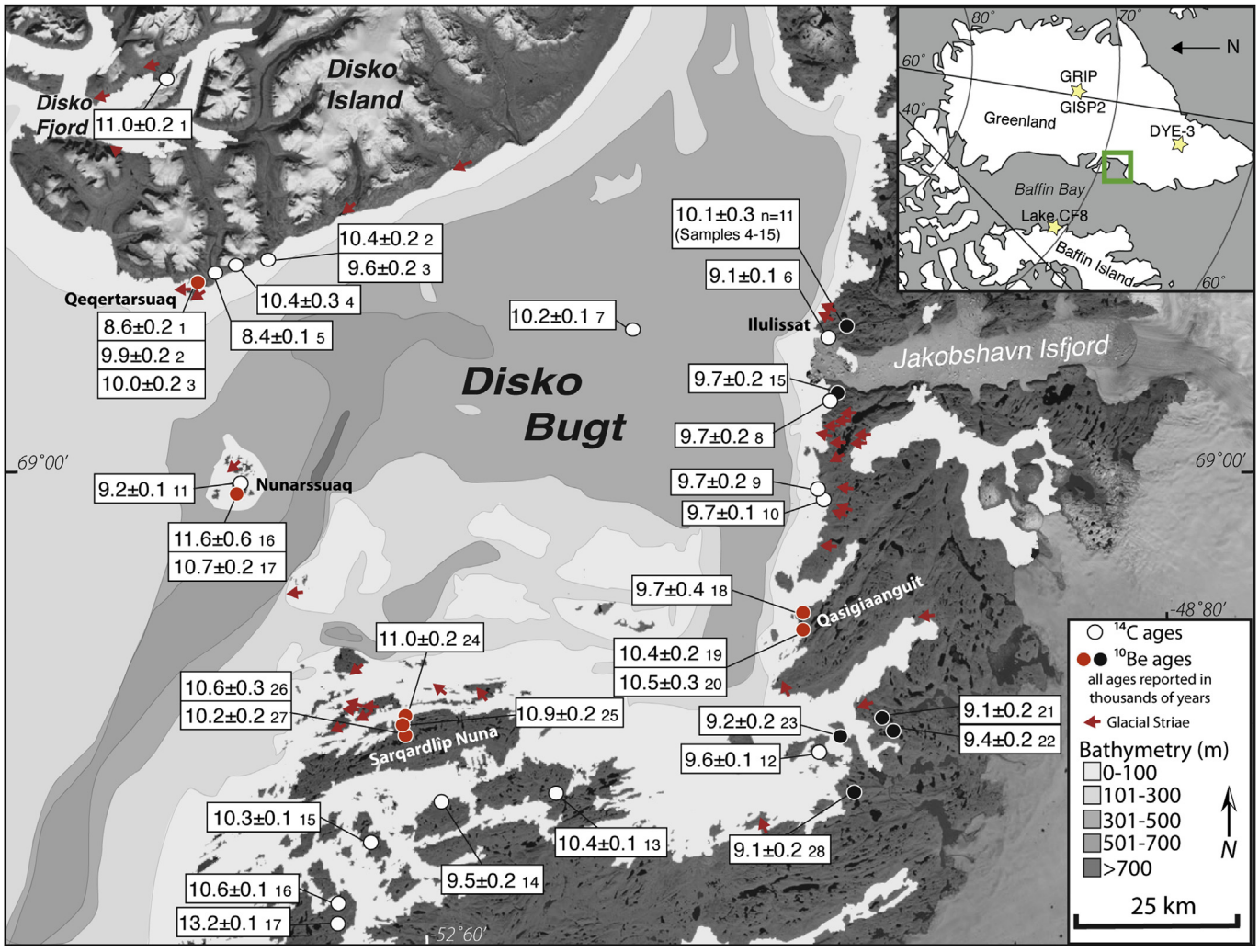

Fig. 1. Disko Bugt region shown in a composite of LANDSAT images; bathymetry from Lloyd et al. (2005) overlain in marine areas, with red arrows denoting past ice flow directions (Christoffersen, 1974). Ages reported in thousands of years (red dots = ^{10}Be ages from this study; black dots = ^{10}Be ages from previous work; white dots = radiocarbon ages); number following age corresponds to sample information in Tables 1–3. Inset shows location of Disko Bugt (green box) within the region, as well as the location of ice cores mentioned in the text. (For interpretation of the references to color in this figure legend, the reader is referred to the web version of this article.)

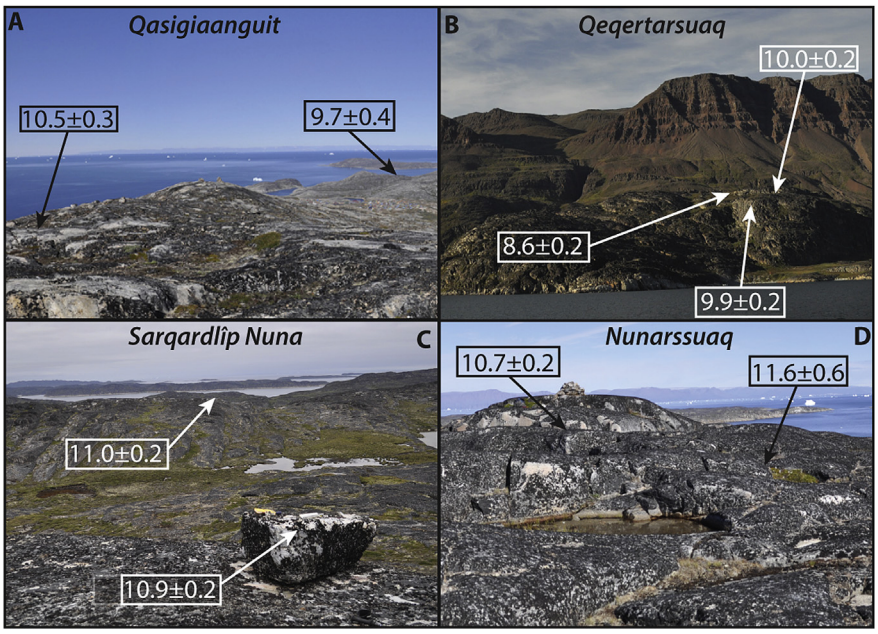

Fig. 2. Sample photos with corresponding ages in thousands of years. (A) View across Qasigiaanguit field site to the WNW toward Disko Bugt with Disko Island in the distance. (B) View to the north of Qeqertarsuaq field site, note crystalline bedrock outcrop below overlying basalt. (C) Boulder perched on bedrock in the foreground: view to the north across the Sarqardîp Nuna field site. (D) View to the north of the two sampled bedrock surfaces at Nunarssuaq, with southern Disko Island in the background.

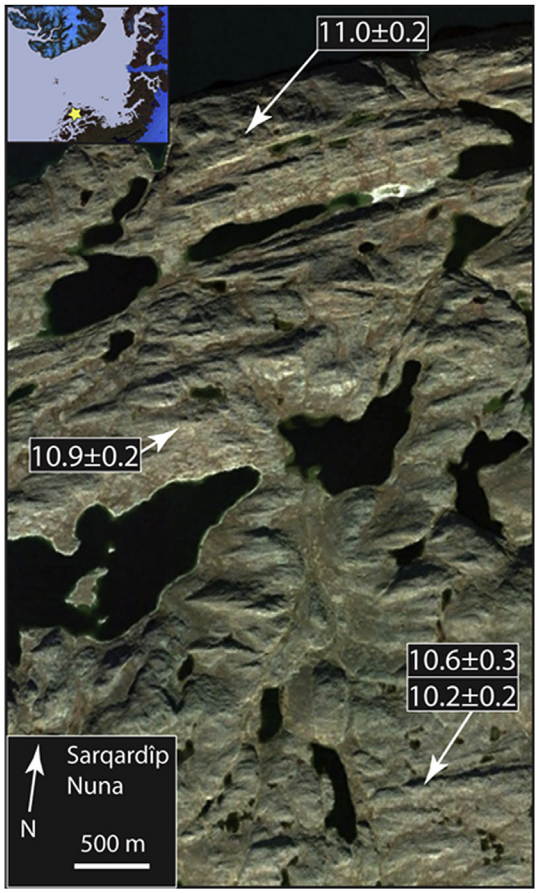

Fig. 3. Satellite image of the sampling transect on Sarqardîp Nuna; ages in thousands of years. Inset map shows the location of the figure (yellow star) within Disko Bugt. (For interpretation of the references to color in this figure legend, the reader is referred to the web version of this article.)

to a chronology of retreat from the western shelf break that began by 13,860 ± 90 cal yr BP (core VC34; Fig. 4; all marine radiocarbon ages are calibrated using MARINECAL09 with a ΔR of 140 ± 25 based on http://calib.qub.ac.uk/marine/ and Lloyd et al. (2011) and are presented as the mean ± half the 1-sigma range; Ó Cofaigh et al., 2013), with a brief, but significant, re-advance at 12,370 ± 210 cal yr BP (core VC20; Fig. 4; Ó Cofaigh et al., 2013). Ice subsequently retreated rapidly eastward from the continental shelf by 10,920 ± 140 cal yr BP (core MSM-343300; Fig. 4; McCarthy, 2011; Hogan et al., 2012). High rates of ice-sheet ablation continued between 10.9 ka and 9.5 ka (Jennings et al., 2013), with ice sheet recession out of Disko Bugt by 10,160 ± 210 cal yr BP (core POR-18; Fig. 1; Lloyd et al., 2005).

The terrestrial chronology constraining retreat of ice from the western margin of Disko Bugt exhibits a wide range of ages (Fig. 1; Table 1). Much of the deglaciation constraints are from minimum-limiting radiocarbon ages derived from marine macrofossils and bulk sediments in lake sediment cores. The oldest of these radiocarbon ages comes from southwest of Disko Bugt, where a minimum age of 13,220 ± 130 cal yr BP was derived from bulk sediment in a lake sediment core (Fredskild, 1996). This age has previously been considered dubious because it is at odds with the existing understanding of the local relative sea level history (Bennike and Björck, 2002). Additional basal ages obtained from bulk lake sediment in the area constrain deglaciation to before 10,550 ± 140, 10,360 ± 120, and 10,330 ± 80 cal yr BP (Long and Roberts, 2003; Long et al., 2003). Bivalves in raised marine deposits (18 m asl), south of Sarqardîp Nuna, constrain deglaciation prior to 9510 ± 220 cal yr BP (Donner and Jungner, 1975). On Nunarssuaq Island, in west-central Disko Bugt, bivalves date to 9190 ± 130 cal yr BP (Bennike et al., 1994), indicating the GrIS had retreated from the mouth of Disko Bugt some time prior to this age.

To the north of Disko Bugt, the deglacial chronology from Disko Island is derived from a basal organic sediment sample in a lake sediment core and numerous shells from raised marine deposits. Geomorphic evidence suggests the possibility of two local advances during what has been termed the Godhavn Stade and Disko Stade.

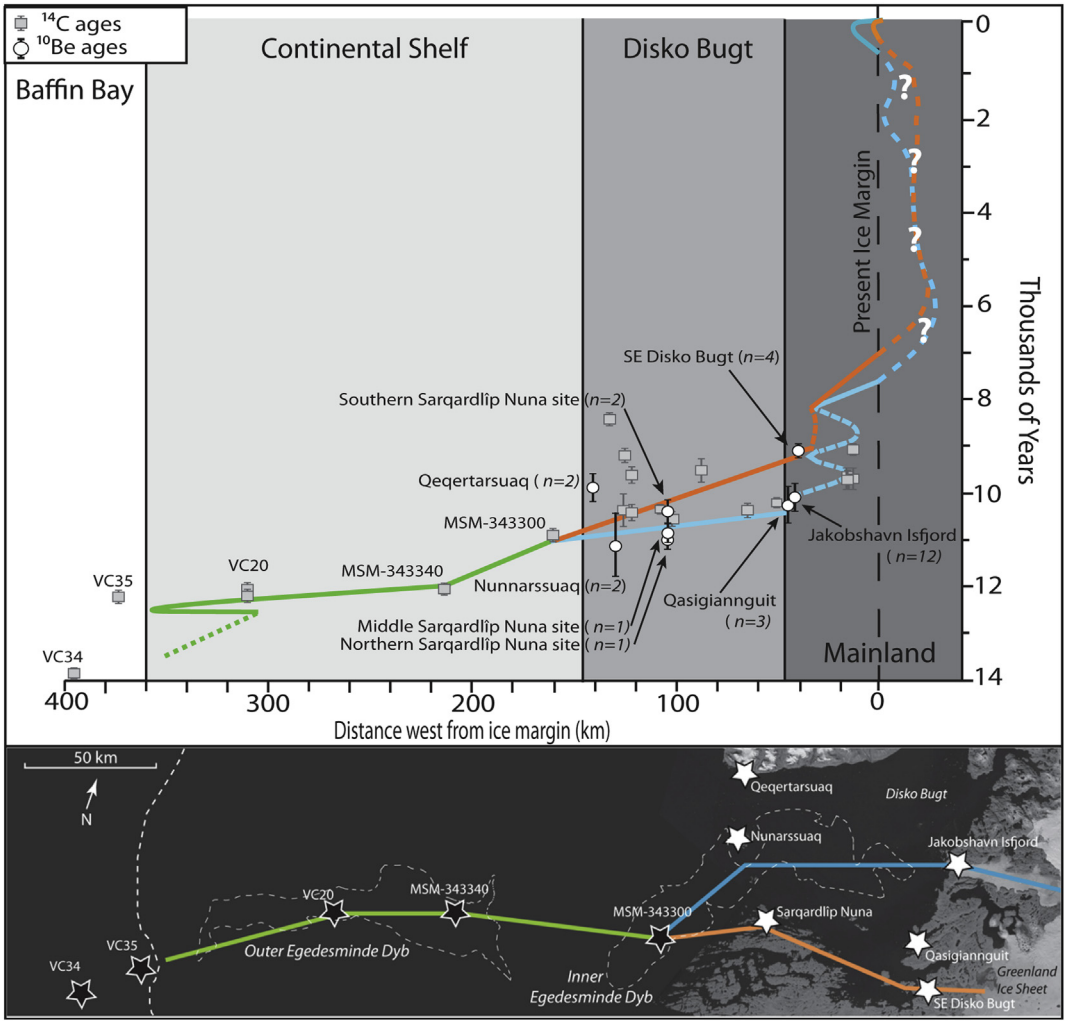

Fig. 4. Top panel: Time-distance diagram of western Greenland ice margin in Disko Bugt region. All ages from Disko Bugt are shown in Fig. 1. Radiocarbon ages from the continental shelf derived from McCarthy (2011), Ó Cofaigh et al. (2013), and (Quillmann et al., 2009). Bottom panel: composite LandSat image depicting the individual transects and locations used in the time-distance diagram as well as in retreat rate calculations. The dotted line represents the 400 m depth contour. (For interpretation of the references to color in this figure legend, the reader is referred to the web version of this article.)

Table 1
Sample information for previously published deglacial radiocarbon ages from Disko Bugt

Sample ID	Ref. to Fig. 1	Latitude (degrees)	Longitude (degrees)	Age (^{14}C yrs BP)	Age (cal yrs BP)[a]	Material	Reference
Beta-183253	1	69.5243	−53.7224	9700 ± 100	11,020 ± 210	Bulk Sediment	Long et al., 2011
K-4567	2	69.3000	−53.2500	9220 ± 130	10,400 ± 150	Shells	Frich and Ingólfsson, 1990
Hel-2210	3	69.3000	−53.2500	9060 ± 120	9610 ± 150	Shells	Frich and Ingólfsson, 1990
AAR-5	4	69.2833	−53.3333	9650 ± 250	10,350 ± 320	Shells	Ingólfsson, 1990
K-3663	5	69.2833	−53.4666	7600 ± 110	8430 ± 110	Shells	Ingólfsson, 1990
Ua-1086	6	69.2000	−51.0667	8795 ± 130	9070 ± 90	Shells	Weidick and Bennike, 2007
AA-37711	7	69.1757	−51.8230	9483 ± 65	10,190 ± 80	Foraminifera	Lloyd, 2005
K-1818	8	69.1000	−51.0667	8630 ± 130	9690 ± 200	Shells	Weidick, 1972
K-2023	9	69.0167	−51.1333	8680 ± 135	9740 ± 180	Shells	Weidick, 1974
Ua-4574	10	69.0000	−51.1167	9180 ± 75	9710 ± 130	Shells	Weidick and Bennike, 2007
RCD-21	11	68.9833	−53.3167	8690 ± 90	9190 ± 130	Mya truncata; Hiatella arctica	Bennike et al., 1994
AA-35659	12	68.6333	−51.1176	8585 ± 86	9570 ± 90	Bulk Sediment	Long and Roberts, 2002
AA-39655	13	68.6170	−52.1101	9180 ± 80	10,360 ± 120	Bulk Sediment	Long et al., 2003
Hel-362	14	68.6000	−52.5666	8970 ± 170	9510 ± 220	Shells	Donner and Jungner, 1975
AA-38844	15	68.5333	−52.9667	9185 ± 62	10,330 ± 80	Bulk Sediment	Long and Roberts, 2003
AA-38842	16	68.4333	−52.8500	9330 ± 99	10,550 ± 140	Bulk Sediment	Long and Roberts, 2003
K-5133	17	68.4333	−52.9500	11,320 ± 140	13,220 ± 130	Bulk Sediment	Fredksild, 1996

Note: K dates are treated as atmospheric samples because they were originally normalized to 0 per mil PDB, the ΔR correction was made after calibration for these samples.
[a] Ages were calibrated using Calib 6.0 and reported as the mean ± 1σ; ages from terrestrial source material are calibrated using INTCAL09; ages from marine source material were calibrated using MARINECAL09 with a ΔR of 140 ± 25 based on http://calib.qub.ac.uk/marine/ and Lloyd et al. (2011).

Table 2
Sample information for previously published ^{10}Be ages.

Ref. to Fig. 1	Sample name	Latitude (N)	Longitude (W)	Elevation (m)	Sample type	Thickness (cm)	Shielding correction	Quartz (g)	^{9}Be (ug)	^{10}Be/^{9}Be ratio	Uncertainty (atoms g^{-1})	^{10}Be (atoms g^{-1})	^{10}Be uncertainty (atoms g^{-1})	^{10}Be age (ka)	Reference
4	GL097	69.2510	−50.8220	470	Boulder	2.0	1.000	16.350	247	6.54E−14	1.70E−15	6.620E+04	1.721E+03	9.6 ± 0.3	Corbett et al., 2011
5	GL096	69.2500	−50.8230	468	Bedrock	3.0	1.000	15.280	247	6.72E−14	1.29E−15	7.270E+04	1.396E+03	10.7 ± 0.2	Corbett et al., 2011
6	JAKN08-21	69.2410	−50.9807	390	Bedrock	1.0	1.000	75.487	154	4.68E−13	2.48E−14	6.388E+04	3.383E+03	10.0 ± 0.5	Young et al., 2011a, Young et al. 2011b
7	JAKN08-22	69.2401	−50.9614	360	Boulder	4.5	1.000	80.162	159	4.49E−13	1.41E−14	5.964E+04	1.868E+03	9.8 ± 0.3	Young et al., 2011a, Young et al. 2011b
8	GL092	69.2300	−50.9020	397	Boulder	1.0	1.000	20.140	248	8.01E−14	1.59E−15	6.590E+04	1.308E+03	10.2 ± 0.2	Corbett et al., 2011
9	GL093	69.2300	−50.9020	397	Bedrock	2.0	1.000	18.940	246	7.71E−14	1.94E−15	6.690E+04	1.683E+03	10.4 ± 0.3	Corbett et al., 2011
10	GL100	69.2270	−50.9300	292	Boulder	2.0	1.000	15.530	247	5.60E−14	1.22E−15	5.950E+04	1.296E+03	10.3 ± 0.2	Corbett et al., 2011
11	GL101	69.2270	−50.9290	295	Bedrock	3.5	1.000	20.190	247	6.87E−14	1.30E−15	5.620E+04	1.063E+03	9.8 ± 0.2	Corbett et al., 2011
12	GL102	69.2070	−51.1340	85	Bedrock	1.0	1.000	19.650	247	5.70E−14	1.27E−15	4.790E+04	1.067E+03	10.2 ± 0.2	Corbett et al., 2011
13	JAKN08-01	69.2055	−51.1244	112	Bedrock	2.5	1.000	80.046	181	3.20E−13	7.85E−15	4.758E+04	1.168E+03	10.0 ± 0.2	Young et al., 2011a, Young et al. 2011b
14	JAKN08-08	69.1993	−50.9474	338	Bedrock	1.0	1.000	85.060	120	6.50E−13	1.83E−14	6.142E+04	1.727E+03	10.1 ± 0.3	Young et al., 2011a, Young et al. 2011b
15	09GRO-01	69.1098	−51.0415	208	Bedrock	5.0	1.000	77.094	102	5.69E−13	1.42E−14	5.025E+04	1.254E+03	9.7 ± 0.2	Young et al., 2011a, Young et al. 2011b
21	10GRO-33	68.7027	−50.8445	328	Bedrock	3.0	0.998	50.040	162	2.50E−13	4.69E−15	5.400E+04	1.010E+03	9.1 ± 0.2	Young et al., 2013a
22	10GRO-34	68.7000	−50.8209	148	Bedrock	2.0	1.000	53.460	162	2.79E−13	5.24E−15	5.670E+04	1.060E+03	9.4 ± 0.2	Young et al., 2013a
23	10GRO-08	68.6695	−50.9987	135	Bedrock	3.5	1.000	58.060	162	2.39E−13	4.57E−15	4.460E+04	8.530E+02	9.2 ± 0.2	Young et al., 2013a
28	10GRO-18	68.6164	−51.0512	180	Bedrock	4.5	1.000	58.780	162	2.51E−13	6.21E−15	4.620E+04	1.140E+03	9.1 ± 0.2	Young et al., 2013a

The Godhavn Stade is expressed as a discontinuous moraine at the mouth of major valleys along the southwestern margin of Disko Island. The age of the Godhavn Stade is constrained by a minimum limiting age from a shell dating to 10,350 ± 320 cal yr BP, and is believed to represent GrIS expansion from Disko Bugt on to Disko Island during the LGM (Ingólfsson et al., 1990). The Disko Stade is an advance of local Disko Island glaciers expressed as a series of moraines near the valley mouth, which truncate Godhavn Stade moraines on eastern Disko Island. The Disko Stade is dated to ~10 ka, and theorized to be the result of changes in the predominant wind direction and moisture source (Ingólfsson et al., 1990), while others suggest that the advance could be attributed to surging local glaciers (Weidick and Bennike, 2007). At the eastern end of Disko Fjord, on western Disko Island, the oldest age constraint of deglaciation is from bulk lake sediments, which place deglaciation prior to 11,020 ± 210 cal yr BP (all terrestrial radiocarbon ages are calibrated using INTCAL09 using http://calib.qub.ac.uk/marine/; Long et al., 2011). Four radiocarbon ages derived from bivalves along the south coast of Disko Island indicate ice-free marine conditions by 10,350 ± 320, 10,400 ± 150, 9610 ± 150, and 8430 ± 110 cal yr BP (Frich and Ingólfsson, 1990; Ingólfsson et al., 1990). Overall, the existing chronology suggests the retreat of ice from Disko Island began at ~11 ka on the western portion of the island, with slightly later retreat occurring along the southern coast at ~10 ka, though it remains unclear whether the chronology pertains to the retreat of the GrIS or retreat of locally sourced glaciers.

The deglacial chronology from eastern Disko Bugt relies on both radiocarbon dating as well as ^{10}Be dating. Radiocarbon ages from near the mouth of Jakobshavn Isfjord yield minimum-limiting constraints on deglaciation of 9070 ± 90 cal yr BP (Weidick and Bennike, 2007) and 9690 ± 2000 cal yr BP (Weidick, 1972). Samples collected ~20 km south of Jakobshavn Isfjord yield similar radiocarbon ages of 9740 ± 180 cal yr BP (Weidick, 1974) and 9710 ± 130 cal yr BP (Weidick and Bennike, 2007). These ages are in agreement with recent ^{10}Be ages, which indicate the landscape near Jakobshavn Isfjord deglaciated at 10.1 ± 0.3 ka ($n = 12$; Corbett et al., 2011; Young et al., 2011a, 2011b, 2013a). In southeastern Disko Bugt, the timing of deglaciation is derived from ^{10}Be ages and radiocarbon ages from a lake sediment core. The core yields a bulk sediment basal age of 9570 ± 90 cal yr BP (Long and Roberts, 2002), and four ^{10}Be ages from nearby average 9.2 ± 0.1 ka (Fig. 1; Young et al., 2013a).

The existing chronology in and around Disko Bugt constrains deglaciation to ~9–11 ka. However, in most places the timing of deglaciation has not been dated directly. The majority of radiocarbon-dated material is of marine origin, and thus relies on a marine reservoir correction based on modern ocean circulation within Disko Bugt (Lloyd et al., 2011), which may differ from the oceanographic conditions during deglaciation. In addition, many of the radiocarbon ages are from bulk lake sediment samples that have been noted in a number of studies to give erroneous old ages (Kaplan et al., 2002; Bennike et al., 2010), or are from marine organisms which colonize the seafloor some unknown period of time following deglaciation. Here, we report twelve new ^{10}Be ages from four new locations around Disko Bugt, which directly date the retreat of ice from the landscape. We compare these new ages to previously published ^{10}Be and ^{14}C ages to improve the chronology of ice retreat out of Disko Bugt during the early Holocene. The additional ^{10}Be ages connect the comprehensive chronologies of early-to-late Holocene ice margin fluctuation on the Greenlandic mainland to emerging records from the continental shelf. The combined time-distance history spans from ~14 ka to present, and from the continental shelf break to the present ice margin.

3. Methods

Samples for ^{10}Be dating were collected from glacially sculpted bedrock surfaces ($n = 8$) and perched erratic boulders ($n = 4$) with a hammer and chisel. Samples were collected from the central portion of boulders and outcrops, away from non-horizontal surfaces, edges, and corners. Latitude, longitude and elevation were collected at all sample locations using a handheld GPS device and topographic shielding was measured using a clinometer. Samples were collected above the local marine limit as indicated by published relative sea level curves (Long and Roberts, 2002, 2003; Long et al., 2006, 2011), and geomorphic evidence such as the presence of raised beaches and washing limits. An exception to this sampling strategy is our collection of samples KE-11-01 and KE-11-02 at ~90 m asl from the highest point on the island of Nunarssuaq, which is below the published marine limit of >95 m for the site (Rasch, 2000). However, local relative sea level curves suggest that rebound was rapid at this time, and thus we expect a negligible age difference for the actual timing of deglaciation and the age of our samples. Nonetheless, ^{10}Be ages from this location should be considered minimum-limiting constraints on the timing of deglaciation.

All samples underwent physical and chemical processing following procedures modified from Kohl and Nishiizumi (1992) at the University at Buffalo Cosmogenic Isotope Laboratory. Samples were crushed and the 425–850 μm size fraction was separated by sieving. Dilute HCl and HNO_3–HF acid treatment and heavy liquid mineral separation were used to isolate quartz. Quartz was digested with a known amount of ^{9}Be carrier and Be was isolated by ion-exchange chromatography and selective precipitation with NH_4OH. ^{10}Be/^{9}Be AMS measurements were performed at Lawrence Livermore National Laboratory and normalized to standard 07KNSTD3110 with a reported ratio of 2.85×10^{-12} (Nishiizumi et al., 2007; Rood et al., 2010). Ratios from process blanks were 6.19×10^{-15} and 1.49×10^{-15}, with AMS precision ranging from 5.4 to 1.8% for blank corrected ^{10}Be/^{9}Be sample ratios.

All ^{10}Be ages (including previously published ages) are calculated using a modified version of the Matlab code developed for the CRONUS-Earth web-based calculator using the regionally calibrated Baffin Bay ^{10}Be production rate of 3.96 ± 0.07 atoms g^{-1} a^{-1} (Young et al., 2013b) and the constant-production scheme of Lal/Stone (Lal, 1991; Stone, 2000) with no corrections made for local isostatic rebound. We use the regionally calibrated Baffin Bay production rate (vs. NENA 10Be production rate of 3.91 ± 0.19 atoms g^{-1} a^{-1}; Balco et al., 2009) because ages calculated with the Baffin Bay rate have been demonstrated to agree with independent local radiocarbon evidence, and the Baffin Bay rate minimizes the systematic error contribution from production-rate uncertainties to our ^{10}Be ages. Sample sites are at local high points on the landscape and are inferred to be windswept, thus no corrections for snow cover have been made. Additionally, glacial polish and striae are abundant on bedrock surfaces throughout the field area, indicating little erosion since ice sheet recession. Thus, we made no corrections for erosion when calculating ^{10}Be ages.

4. Results and interpretation

We calculate twelve ^{10}Be ages from glacially sculpted bedrock surfaces ($n = 8$) and perched erratic boulders ($n = 4$). Two ages from bedrock samples collected ~10 m apart on Nunarssuaq are 11.6 ± 0.6 ka and 10.7 ± 0.2 ka and average 11.1 ± 0.7 ka (Figs. 1 and 2; Table 3; all averages are the mean ± one standard deviation). Although it is possible that the older age may reflect inherited ^{10}Be from previous exposures, these two ages from the same site overlap at 2-sigma so we opt to calculate their average. At Qeqertarsuaq,

Table 3
Sample information for ^{10}Be ages.

Ref. to Fig. 1	Sample name	Latitude (N)	Longitude (W)	Elevation (m)	Sample type	Thickness (cm)	Shielding correction	Quartz (g)	^{9}Be (ug)	^{10}Be/^{9}Be ratio	Uncertainty (atoms g^{-1})	^{10}Be (atoms g^{-1})	^{10}Be uncertainty (atoms g^{-1})	^{10}Be age (ka)
Qeqertarsuaq														
1	DISKO-03	69.2637	−53.5548	173	Bedrock	3.0	0.992	60.0600	162	2.39E−13	4.59E−15	4.32E+04	8.30E+02	8.6 ± 0.2
2	DISKO-01	69.2624	−53.5521	150	Bedrock	3.0	0.992	50.0373	162	2.23E−13	4.21E−15	4.84E+04	9.12E+02	9.9 ± 0.2
3	DISKO-02	69.2621	−53.5508	153	Boulder	3.0	0.992	60.2046	162	2.73E−13	5.26E−15	4.92E+04	9.47E+02	10.0 ± 0.2
Nunarssuaq														
16	KE-11-01	68.9845	−53.3337	89	Bedrock	3.0	1.000	40.7844	283	1.15E−13	6.23E−15	5.36E+04	2.89E+03	11.6 ± 0.6
17	KE-11-02	68.9843	−53.3337	87	Bedrock	1.0	1.000	50.0042	285	1.31E−13	2.72E−15	5.00E+04	1.04E+03	10.7 ± 0.2
Qasigiaanguit														
18	QA-11-05	68.8473	−51.1676	195	Boulder	2.5	1.000	25.1527	286	6.68E−14	3.02E−15	5.08E+04	2.30E+03	9.7 ± 0.4
19	QA-11-02	68.8106	−51.1400	420	Bedrock	3.0	1.000	49.8469	284	1.77E−13	3.23E−15	6.75E+04	1.23E+03	10.4 ± 0.2
20	QA-11-01	68.8046	−51.1552	360	Bedrock	3.0	1.000	50.1276	285	1.70E−13	4.07E−15	6.47E+04	1.55E+03	10.5 ± 0.3
Sarqardîp Nuna														
24	SN-11-07	68.6931	−52.6969	119	Boulder	1.5	1.000	41.5965	224	1.49E−13	2.80E−15	5.34E+04	1.01E+03	11.0 ± 0.2
25	SN-11-02	68.6725	−52.7072	119	Boulder	2.0	1.000	40.5716	224	1.42E−13	2.69E−15	5.26E+04	9.93E+02	10.9 ± 0.2
26	SN-11-04	68.6491	−52.6664	220	Bedrock	3.0	1.000	32.5778	284	9.65E−14	2.31E−15	5.64E+04	1.35E+03	10.6 ± 0.3
27	SN-11-05	68.6491	−52.6649	221	Boulder	2.0	1.000	50.1188	286	1.44E−13	3.39E−15	5.50E+04	1.29E+03	10.2 ± 0.2

Notes: All samples were spiked with a 405.4 μg/g ^{9}Be carrier except SN-11-02 which were spiked with a 372.5 μg/g ^{9}Be carrier; AMS results are standardized to 07KNSTD; ratios are blank-corrected, and shown at 1-sigma uncertainty.

southern Disko Island, one sample from a boulder yields an age of 8.6 ± 0.2 ka, and two bedrock samples yield ages of 9.9 ± 0.2 ka and 10.0 ± 0.2 ka (Figs. 1 and 2; Table 3). We consider the age of 8.6 ± 0.2 ka as an outlier because it is much younger than the other two ^{10}Be ages, as well as a radiocarbon age of 10.4 ± 0.3 ka derived from marine bivalves collected ~5 km to the east (Ingólfsson et al., 1990). Thus, the two ages from the Qeqertarsuaq site average 10.0 ± 0.1 ka. On the southern margin of Disko Bugt, on the island of Sarqardîp Nuna, four ^{10}Be ages are calculated from samples collected at three sites along transect extending 5 km to the south from the northern coast of the island (Fig. 3). A boulder sample from the northernmost site yields a ^{10}Be age of 11.0 ± 0.2 ka (Figs. 1 and 2; Table 3). To the south, a boulder sample collected at the middle site of the transect provides a ^{10}Be age of 10.9 ± 0.2 ka (Figs. 1 and 2; Table 3). At the southernmost transect site, bedrock and boulder samples located ~10 m apart yield ^{10}Be ages of 10.6 ± 0.3 ka and 10.2 ± 0.2 ka, respectively (Figs. 1 and 2; Table 3); the average age from the southernmost site is 10.4 ± 0.3 ka. At Qasigiaanguit, in eastern Disko Bugt, 40 km south of Jakobshavn Isfjord, ^{10}Be ages derived from two bedrock samples and one boulder sample are 10.5 ± 0.3 ka, 10.4 ± 0.2 ka, and 9.7 ± 0.4 ka respectively. The younger of these ages, 9.7 ± 0.4 ka, is from a sample collected at ~200 m lower in elevation than the older two samples (Table 3). The difference in ages may reflect thinning of the ice margin at this location during deglaciation. However, for an age of deglaciation of the Qasigiaanguit area we use an average age of 10.2 ± 0.4 ka (n = 3; Figs. 1 and 2; Table 3).

5. Discussion

5.1. Deglaciation of Disko Bugt

Samples collected from four localities on the perimeter of Disko Bugt, combined with previously published ^{10}Be ages from the eastern coast of Disko Bugt, outline a pattern of initial ice retreat out of central Disko Bugt with later recession along the margins. The oldest ^{10}Be ages are from Nunarssuaq, where two ages average 11.1 ± 0.7 ka and provide a closer constraint on deglaciation than a minimum limiting radiocarbon age of 9190 ± 130 cal yr BP from the site (Fig. 1; Bennike et al., 1994). A similar age of 11.0 ± 0.2 ka was determined for the northernmost site (most proximal to Disko Bugt) in the Sarqardîp Nuna transect. The remaining ages from the Sarqardîp Nuna transect decrease in age toward the south. Radiocarbon ages from south of Sarqardîp Nuna range from 10,550 ± 140 to 9510 ± 220 cal yr BP (n = 4; Fig. 1; Donner and Jungner, 1975; Long and Roberts, 2003) and further corroborate ice recession occurring later to the south of Disko Bugt than in central Disko Bugt.

On southern Disko Island at Qeqertarsuaq ^{10}Be ages that average 10.0 ± 0.1 ka (n = 2) indicate later deglaciation than in central-western and central-southern Disko Bugt. One interpretation for these younger ages is that ice lingered on Disko Island following recession of the GrIS from Disko Bugt, fed by local ice caps on the high plateaus covering much of Disko Island. It is also possible that the relatively young ^{10}Be ages is evidence of the Disko Stade advance (Ingólfsson et al., 1990), although no other evidence of the Disko Stade advance has been found on western Disko Island. Our ^{10}Be ages overlap within error with radiocarbon ages from the southern coast of Disko Island that range from 10,400 ± 150 to 8430 ± 110 cal yr BP (n = 4; Fig. 1; Frich and Ingólfsson, 1990; Ingólfsson et al., 1990).

At Qasigiaanguit, in eastern Disko Bugt, the average ^{10}Be age of 10.2 ± 0.4 ka (n = 3; Fig. 1) overlaps within error with the average ^{10}Be age of deglaciation from the Ilulissat area of 10.1 ± 0.3 ka (n = 12; Corbett et al., 2011; Young et al., 2013a) and is older than ^{10}Be ages constraining deglaciation in southeastern Disko Bugt at 9.2 ± 0.1 ka (n = 4; Young et al., 2013a). The ages from eastern Disko Bugt suggest that deglaciation in east-central Disko Bugt occurred first, and then later in southeastern Disko Bugt. Radiocarbon ages of 9740 ± 180 and 9710 ± 1300 cal yr BP (Weidick, 1974; Weidick and Bennike, 2007) from 25 km north of Qasigiaanguit, and 9570 ± 90 cal yr BP (Long and Roberts, 2002) from 20 km south of Qasigiaanguit, provide minimum limiting constraints on deglaciation and support our ^{10}Be ages. A sedimentological shift observed in a marine sediment core from offshore of Disko Bugt indicates a pronounced decrease in ice-rafted debris at ~10 ka (core MSM-343340), and correlates to the time when ice retreated out of east-central Disko Bugt and onto the mainland (McCarthy, 2011).

The pattern of ages suggests ice receded out of central Disko Bugt first near Jakobshavn Isfjord, with the timing of ice recession later along the mainland south of Disko Bugt. The spatial pattern of ice retreat may be explained in part by the bathymetric configuration of Disko Bugt (Fig. 1), with more rapid ice retreat occurring in areas of deeper water in central Disko Bugt. Here, ice may have been more vulnerable to collapse as it retreated into deeper water with a widening bay geometry (Nick et al., 2010; Enderlin et al., 2013). Conversely, ice retreat may have been slower along southern Disko Bugt as the ice resided in relatively shallow water. This conceptual model of deglaciation is corroborated by acoustic profiles from Disko Bugt. The lack of significant sediment accumulation in the western and central bay suggests that central Disko Bugt deglaciated rapidly without major standstills or re-advances (Hogan et al., 2012).

5.2. Retreat rates

Ice-margin retreat rates through Disko Bugt can be estimated from our ^{10}Be chronology. We calculate maximum and minimum possible retreat scenarios based on the average age of deglaciation with full consideration of the standard deviation of the average age at strategic locations. We exclude the Disko Island ages from the calculation of GrIS retreat rates, as our ages from Disko Island may constrain the retreat of locally sourced glaciers rather than that of the GrIS. The retreat of the GrIS margin 90 km from western Disko Bugt (10.8 ± 0.5; n = 6) to eastern Disko Bugt (9.9 ± 0.5; n = 19) yields rates that range from instantaneous (beyond the resolution of our ^{10}Be chronology) to 50 m a^{-1}. However, closer inspection of the ^{10}Be chronology demonstrates that the GrIS retreated onto land later along the southeastern margin of Disko Bugt, while the retreat of ice onto land occurred earlier the Jakobshavn and Qasigiaanguit areas. The spatial variability in the retreat rate is further examined by sub-dividing Disko Bugt into a southern and central section (Fig. 4). Retreat of 90 km in the central section of Disko Bugt, from Nunarssuaq and the northern site at Sarqardlîp Nuna (11.1 ± 0.5; n = 3) to the eastern coast of Disko Bugt at Jakobshavn Isfjord and Qasigiaanguit (10.1 ± 0.3; n = 15) occurred at a rate of between ~50 and 450 m a^{-1}. In contrast, the GrIS receded the 70 km from the southern site at Sarqardlîp Nuna (10.4 ± 0.3 n = 2) to southeastern Disko Bugt (9.2 ± 0.1; n = 4) at a rate between ~50 and 70 m a^{-1}.

Our compilation of ^{10}Be and radiocarbon ages reveals rapid retreat of the GrIS margin through Disko Bugt. Retreat rates ranging from ~50 to 450 m a^{-1} for central Disko Bugt overlaps the range of 22–275 m a^{-1} retreat rates reported from the nearby continental shelf (Ó Cofaigh et al., 2013) following a re-advance at 12.3 ka, and is equal to or faster than the ~100 m a^{-1} reconstructed for the deglaciation of Jakobshavn Isfjord during the middle Holocene (Young et al., 2011b). Ice retreat through Disko Bugt is also estimated to be equal to or faster than at Sermilik Fjord in southeast Greenland (≥80 m a^{-1}; Hughes et al., 2012) and at Sam Ford Fjord on Baffin Island (>58 m a^{-1}; Briner et al., 2009). On the west coast

of Norway, Mangerud et al. (2013) estimate retreat rates of 240–370 m a^{-1}, and suggest that this is near the maximum possible retreat rates in a long fjord system. If retreat rates within central Disko Bugt are at the upper end of the range we calculate then they may have been faster than rates reported for other fjord systems, and may have even resembled the rapid break-up of ice shelves in the western Antarctica Peninsula (Scambos et al., 2004).

5.3. Deglaciation from the continental shelf to the present ice margin

In this section, we describe the reconstruction of a time-distance history of the western GrIS in the Disko Bugt region from the continental shelf break to the present ice margin (Fig. 4). The earliest constraints on deglaciation of the western margin of the GrIS are from marine sediment cores collected from trough mouth fans at the edge of the continental shelf (Ó Cofaigh et al., 2013). These cores reveal that GrIS retreat from the continental shelf initiated by 13,860 ± 90 cal yr BP (core VC34; Ó Cofaigh et al., 2013). Following a re-advance at 12,230 ± 130 cal yr BP (core VC20; Ó Cofaigh et al., 2013), the ice margin continued to retreat across the continental shelf with recession off the inner shelf occurring by 10,920 ± 140 cal yr BP (Fig. 3; MSM-343300; Quillmann et al., 2009).

The timing of western Disko Bugt deglaciation at 10.8 ± 0.5 ka is similar to an age on deglaciation of 10,920 ± 140 cal yr BP from the nearby continental shelf (60 km southwest; core MSM-343300; Quillmann et al., 2009). This similarity implies little pause, or slowdown, during deglaciation from the western Greenland shelf and into Disko Bugt. Following ice retreat out of Disko Bugt, the GrIS deposited the Fjord Stade moraines during re-advances at 9.3 and 8.2 ka (Weidick and Bennike, 2007; Young et al., 2011a, 2013a). Following these re-advances, the GrIS retreated to a location at or behind its latest Holocene ice margin by ~7.4 ka near Jakobshavn Isfjord and ~7.0 ka in southeastern Disko Bugt (Young et al., 2011b, 2013a). The GrIS remained behind its present margin throughout the middle Holocene, and radiocarbon-dated lake sediments from a threshold lake basin reveal that the GrIS achieved its minimum mid-Holocene extent at or by 5770 ± 110 cal yr BP (Briner et al., 2010). At Jakobshavn Isfjord, the GrIS was approaching the latest Holocene configuration by ~2.3 ka, achieved its late Holocene maximum around 0.4 ka (Briner et al., 2010), and began retreating by 1850 AD (Csatho et al., 2008). In southeast Disko Bugt, the ice margin neared its latest Holocene maximum position by ~0.3 ka, and culminated in its maximum extent during the late 20th century (Kelley et al., 2012).

5.4. Forcing mechanisms

In evaluating possible forcing mechanisms for rapid retreat of the GrIS from Disko Bugt, two end member scenarios are possible: 1) the retreat of the GrIS was climatically driven by increasing air and ocean temperatures, and 2) ice dynamic factors independent of climatic forcing drove the recession. Retreat of the GrIS from Disko Bugt occurred during a period of ocean and climatic warming, as well as ice sheet thinning. Arctic summer temperatures on Baffin Island (~600 km west) increased 2–4 °C between 11 and 10 ka (Fig. 5; Axford et al., 2009). In addition, evidence of relatively warm Atlantic-derived water reaching northern Baffin Bay just after 10.9 ka implies increased advection of Atlantic water into Baffin Bay around the time of ice retreat from Disko Bugt (Knudsen et al., 2008). Further evidence of a warming Baffin Bay is derived from the presence of driftwood in southwest Greenland dated to 10.8 ± 0.4 ka indicating ice free conditions for part of the year (Weidick, 1975). Estimates of ice sheet elevation change from the

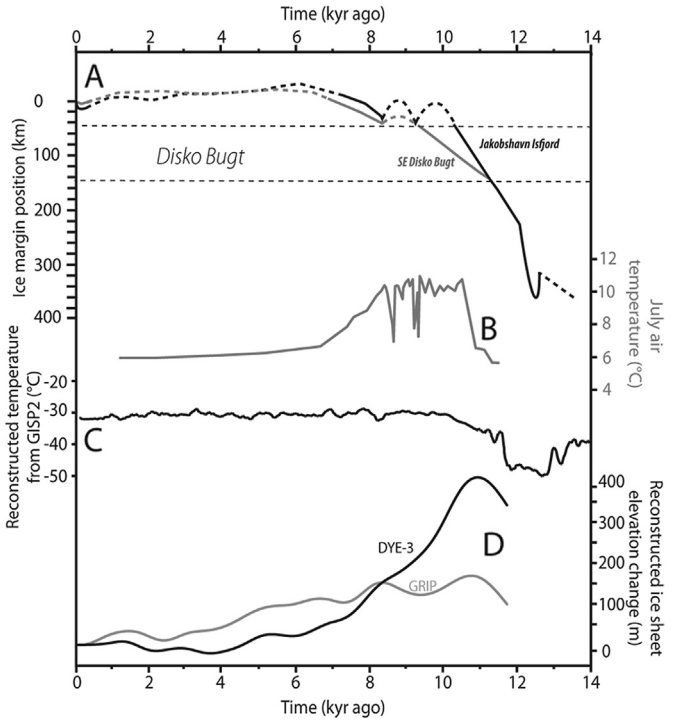

Fig. 5. A) Time-distance diagram presented in Fig. 4, depicting the location of the GrIS margin in the Disko Bugt region since 14 ka; B) Summer air temperature reconstruction from Lake CF8 on Baffin Island, Arctic Canada (Axford et al., 2009); C) Reconstructed temperature from the GISP2 ice core (Alley, 2000); D) ice sheet elevation changes at the GRIP and DYE-3 sites (Vinther et al., 2009).

GRIP and DYE-3 ice cores indicate that accelerated thinning of the GrIS occurred between 11 and 10 ka (Fig. 5; Vinther et al., 2009). This evidence of ameliorating climate provides a possible mechanism for GrIS retreat during the early Holocene.

Evidence for the role of ice dynamics on ice sheet retreat comes from a comparison of the deglaciation of the Disko Bugt area to that of the Uummannaq Fjord system and cross-shelf trough to the north (~220 km). A major difference between the two glacier systems is their geometry, with Disko Bugt exhibiting a widening and bathymetrically deepening geometry from west to east, while Uummannaq is much narrower and bathymetrically deeper, with numerous islands (McCarthy, 2011). Recent investigations of the Uummannaq trough suggest that deglaciation commenced from the continental shelf at ~14.8 ka, ~1000 years earlier than offshore of Disko Bugt (Ó Cofaigh et al., 2013; Roberts et al., 2013). Ice sheet retreat also progressed differently between the two systems, with the ice sheet well within the main fjord at Uummannaq by 12.4 ka, into the inner fjords by 10.8 ka and likely behind its present position at Store Gletscher by 8.7 ka (Roberts et al., 2013). This asynchronous initiation and evolution of ice sheet retreat between the two neighboring systems suggests a local ice dynamic influence on ice sheet recession.

We postulate that climatic factors created a situation in Disko Bugt where the western margin of the GrIS became more susceptible to rapid retreat driven by ice dynamics. As the GrIS thinned, buoyancy may have increased, and was exacerbated by basal melt due to contact with warming ocean water. As buoyancy of the marine-based section of the GrIS increased, the margin may have lost contact with the bathymetric high spanning the mouth of Disko Bugt, which acted as a pinning point. This change could have led to accelerated calving as the basin geometry widens from west to east, prompting rapid recession of the ice margin from deep,

central Disko Bugt to a more stable configuration along southern and eastern coasts of Disko Bugt (Enderlin et al., 2013). This proposed scenario is supported by sedimentological data from the marine cores that suggest calving was a major factor in the early Holocene retreat of the GrIS from the continental shelf (Jennings et al., 2013).

6. Conclusions

New ^{10}Be ages from around Disko Bugt, western Greenland, place the deglaciation of western Disko Bugt at 10.8 ± 0.5 ka, with the ice margin reaching the eastern coast of Disko Bugt near Ilulissat at 10.1 ± 0.3 ka and in southeastern Disko Bugt at 9.2 ± 0.1 ka. This chronology yields a retreat rate between ~50 and 450 m a^{-1} across central Disko Bugt. This rate indicates that ~25% of the overall retreat between the shelf edge and the current position occurred in as little as 700 years. We suggest this retreat was the result of internal ice dynamics acting upon an ice sheet driven out of equilibrium by climatic factors. These findings further emphasize the ability of marine sectors of ice sheets to change rapidly due to ice dynamics in warming climates (e.g. Kjær et al., 2012). Our chronology fills a gap in the current understanding of the early Holocene behavior of the GrIS in Disko Bugt, and provides a dataset that completes a history of a western GrIS margin spanning from the continental shelf to the present ice position, and from the latest Pleistocene through the Holocene.

Acknowledgments

This work greatly benefitted from high precision ^{10}Be measurements from Lawrence Livermore National Laboratory by Susan Zimmerman and Robert Finkel. We appreciate laboratory assistance from Michael Badding and Sarah Lavin. We are grateful for the reviews of A. Jennings and A. Hughes, whose comments improved this manuscript. This research was funded by a Geologic Society of America graduate student grant and grant NSF-1156361 from the U.S. National Science Foundation Program of Geography and Spatial Science.

Appendix A. Supplementary data

Supplementary data related to this article can be found at http://dx.doi.org/10.1016/j.quascirev.2013.09.018.

References

Alley, R.B., 2000. The Younger Dryas cold interval as viewed from central Greenland. Quat. Sci. Rev. 19, 213–226.
Axford, Y., Briner, J.R., Miller, G.H., Francis, D.R., 2009. Paleoecological evidence for abrupt cold reversals during peak Holocene warmth on Baffin Island, Arctic Canada. Quat. Res. 71, 142–149.
Balco, G., Briner, J.P., Finkel, R., Rayburn, J.A., Ridge, J.C., Schaefer, J.M., 2009. Regional beryllium-10 production rate calibration for late-glacial northeastern North America. Quat. Geochronol. 4, 93–107.
Bennike, O., Hansen, K.B., Knudsen, K.L., Penney, D.N., Rasmussen, K.L., 1994. Quaternary marine stratigraphy and geochronology in central West Greenland. Boreas 23, 194–215.
Bennike, O., Anderson, N.J., McGowan, S., 2010. Holocene palaeoecology of southwest Greenland inferred from macrofossils in sediments of an oligosaline lake. J. Paleolimnol. 43, 787–798.
Bennike, O., Björck, S., 2002. Chronology of the last recession of the Greenland Ice Sheet. J. Quat. Sci. 17, 211–219.
Bindschadler, R.A., 1984. Jakobshavns Glacier drainage basin: a balance assessment. J. Geophys. Res. Oceans (1978–2012) 89, 2066–2072.
Bjørk, A.A., Kjær, K.H., Korsgaard, N.J., Khan, S.A., Kjeldsen, K.K., Andresen, C.S., Larsen, N.K., Funder, S., 2012. An aerial view of 80 years of climate-related glacier fluctuations in southeast Greenland. Nat. Geosci. 5, 427–432.
Box, J.E., 2002. Survey of Greenland instrumental temperature records: 1873–2001. Int. J. Climatol. 22, 1829–1847.
Briner, J.P., Bini, A.C., Anderson, R.S., 2009. Rapid early Holocene retreat of a Laurentide outlet glacier through an Arctic fjord. Nat. Geosci 2, 496–499.
Briner, J., Stewart, H., Young, N., Philipps, W., Losee, S., 2010. Using proglacial-threshold lakes to constrain fluctuations of the Jakobshavn Isbræ ice margin, western Greenland, during the Holocene. Quat. Sci. Rev. 29, 3861–3874.
Chalmers, J., Pulvertaft, T., Marcussen, C., Pedersen, A., 1999. New insight into the structure of the Nuussuaq Basin, central West Greenland. Mar. Petrol. Geol. 16, 197–224.
Christoffersen, M., 1974. Quaternary Map of Greenland: Søndre Strømfjord-Nûgssuaq Kvartærgeologisk. Sheet 3, Quaternary Map of Greenland. Greenland Geologic Survey, Copenhagen, Denmark.
Corbett, L.B., Young, N.E., Bierman, P.R., Briner, J.P., Neumann, T.A., Rood, D.H., Graly, J.A., 2011. Paired bedrock and boulder ^{10}Be concentrations resulting from early Holocene ice retreat near Jakobshavn Isfjord, western Greenland. Quat. Sci. Rev. 30, 1739–1749.
Csatho, B., Schenk, T., Van der Veen, C., Krabill, W.B., 2008. Intermittent thinning of Jakobshavn Isbræ, West Greenland, since the Little Ice Age. J. Glaciol. 54, 131–144.
Donner, J., Jungner, H., 1975. Radiocarbon dating of shells from marine Holocene deposits in the Disko Bugt area, West Greenland. Boreas 4, 25–45.
Enderlin, E., Howat, I., Vieli, A., 2013. High sensitivity of tidewater outlet glacier dynamics to shape. Cryosphere Discuss. 7, 551–572.
Fisher, D., Zheng, J., Burgess, D., Zdanowicz, C., Kinnard, C., Sharp, M., Bourgeois, J., 2012. Recent melt rates of Canadian arctic ice caps are the highest in four millennia. Global Planet. Change 84–85, 3–7.
Fredskild, B., 1996. Holocene Climatic Changes in Greenland. The Paleo-eskimo Cultures of Greenland. Danish Polar Center, Copenhagen, pp. 243–251.
Frich, P., Ingólfsson, O., 1990. Det holocæne sedimentationsmiljø ved Igpik samt en model for den relative landhævning i Disko Bugt området, Vestgrønland. In: AÊrsskrift for Dansk Geologisk Forening 1987, vol. 89, pp. 1–10.
Funder, S.V., Hansen, L., 1996. The Greenland ice sheet-a model for its culmination and decay during and after the last glacial maximum. Geol. Soc. Den. Bull. 42, 137–152.
Hogan, K., Dowdeswell, J., Cofaigh, C., 2012. Glacimarine sedimentary processes and depositional environments in an embayment fed by West Greenland ice streams. Mar. Geol. 311–314, 1–16.
Hughes, A.L., Rainsley, E., Murray, T., Fogwill, C.J., Schnabel, C., Xu, S., 2012. Rapid response of Helheim Glacier, southeast Greenland, to early Holocene climate warming. Geology 40, 427–430.
Ingólfsson, Ó., Frich, P., Funder, S., Humlum, O., 1990. Paleoclimatic implications of an early Holocene glacier advance on Disko Island, West Greenland. Boreas 19, 297–311.
Jennings, A., Walton, M.E., Cofaigh, C.Ó., Kilfeather, A., Andrews, J.T., Ortiz, J., De Vernal, A., Dowdeswell, J.A., 2013. Paleoenvironments during the Younger Dryas-early Holocene retreat of the Greenland Ice Sheet from outer Disko Trough, central west Greenland. Journal of Quaternary Science 28, http://dx.doi.org/10.1002/jqs.2652.
Joughin, I., Smith, B.E., Howat, I.M., Scambos, T., Moon, T., 2010. Greenland flow variability from ice-sheet-wide velocity mapping. J. Glaciol. 56, 415–430.
Kaplan, M.R., Wolfe, A.P., Miller, G.H., 2002. Holocene environmental variability in southern Greenland inferred from lake sediments. Quat. Res. 58, 149–159.
Kaufman, D.S., Schneider, D.P., McKay, N.P., Ammann, C.M., Bradley, R.S., Briffa, K.R., Miller, G.H., Otto-Bliesner, B.L., Overpeck, J.T., Vinther, B.M., 2009. Recent warming reverses long-term Arctic cooling. Science 325, 1236–1239.
Kelley, S.E., Briner, J.P., Young, N.E., Babonis, G.S., Csatho, B., 2012. Maximum late Holocene extent of the western Greenland Ice Sheet during the late 20th century. Quat. Sci. Rev. 56, 89–98.
Kjær, K.H., Khan, S.A., Korsgaard, N.J., Wahr, J., Bamber, J.L., Hurkmans, R., van den Broeke, M., Timm, L.H., Kjeldsen, K.K., Bjørk, A.A., 2012. Aerial photographs reveal Late-20th-century dynamic ice loss in Northwestern Greenland. Science 337, 569–573.
Knudsen, K.L., Stabell, B., Seidenkrantz, M.S., Eiriksson, J., Blake, W., 2008. Deglacial and Holocene conditions in northernmost Baffin Bay: sediments, foraminifera, diatoms and stable isotopes. Boreas 37, 346–376.
Lal, D., 1991. Cosmic-ray labeling of erosion surfaces: in situ nuclide production rates and erosion models. Earth Planet. Sci. Lett. 104, 424–439.
Levy, L.B., Kelly, M.A., Howley, J.A., Virginia, R.A., 2012. Age of the Ørkendalen moraines, Kangerlussuaq, Greenland: constraints on the extent of the southwestern margin of the Greenland Ice Sheet during the Holocene. Quat. Sci. Rev. 52, 1–5.
Lloyd, J., Park, L., Kuijpers, A., Moros, M., 2005. Early Holocene palaeoceanography and deglacial chronology of Disko Bugt, west Greenland. Quat. Sci. Rev. 24, 1741–1755.
Lloyd, J., Moros, M., Perner, K., Telford, R.J., Kuijpers, A., Jansen, E., McCarthy, D., 2011. A 100 yr record of ocean temperature control on the stability of Jakobshavn Isbrae, West Greenland. Geology 39, 867–870.
Long, A.J., Roberts, D.H., 2002. A revised chronology for the 'Fjord Stade' moraine in Disko Bugt, west Greenland. J. Quat. Sci. 17, 561–579.
Long, A.J., Roberts, D.H., 2003. Late Weichselian deglacial history of Disko Bugt, West Greenland, and the dynamics of the Jakobshavns Isbrae ice stream. Boreas 32, 208–226.
Long, A.J., Roberts, D.H., Rasch, M., 2003. New observations on the relative sea level and deglacial history of Greenland from Innaarsuit, Disko Bugt. Quat. Res. 60, 162–171.
Long, A., Roberts, D., Dawson, S., 2006. Early Holocene history of the west Greenland Ice Sheet and the GH-8.2 event. Quat. Sci. Rev. 25, 904–922.

Long, A.J., Woodroffe, S.A., Roberts, D.H., Dawson, S., 2011. Isolation basins, sea-level changes and the Holocene history of the Greenland Ice Sheet. Quat. Sci. Rev. 30, 3748–3768.
Mangerud, J., Goehring, B.M., Lohne, Ø.S., Svendsen, J.I., Gyllencreutz, R., 2013. Collapse of marine-based outlet glaciers from the Scandinavian Ice Sheet. Quat. Sci. Rev. 67, 8–16.
Maslanik, J., Stroeve, J., Fowler, C., Emery, W., 2011. Distribution and trends in Arctic sea ice age through spring 2011. Geophys. Res. Lett. 38, L13502.
McCarthy, D.J., 2011. Late Quaternary Ice-ocean Interactions in Central West Greenland. Deptment of Geography, Durham University, Durham, UK, p. 292.
Meier, M.F., Dyurgerov, M.B., Rick, U.K., O'Neel, S., Pfeffer, W.T., Anderson, R.S., Anderson, S.P., Glazovsky, A.F., 2007. Glaciers dominate eustatic sea-level rise in the 21st century. Science 317, 1064–1067.
Miller, G.H., Brigham-Grette, J., Alley, R.B., Anderson, L., Bauch, H.A., Douglas, M.S.V., Edwards, M.E., Elias, S.A., Finney, B.P., Fitzpatrick, J.J., Funder, S.V., Herbert, T.D., Hinzman, L.D., Kaufman, D.S., MacDonald, G.M., Polyak, L., Robock, A., Serreze, M.C., Smol, J.P., Spielhagen, R., White, J.W.C., Wolfe, A.P., Wolff, E.W., 2010. Temperature and precipitation history of the Arctic. Quat. Sci. Rev. 29, 1679–1715.
Möller, P., Larsen, N.K., Kjær, K.H., Funder, S., Schomacker, A., Linge, H., Fabel, D., 2010. Early to middle Holocene valley glaciations on northernmost Greenland. Quat. Sci. Rev. 29, 3379–3398.
Nick, F., Van der Veen, C., Vieli, A., Benn, D., 2010. A physically based calving model applied to marine outlet glaciers and implications for the glacier dynamics. J. Glaciol. 56, 781–794.
Nishiizumi, K., Imamura, M., Caffee, M.W., Southon, J.R., Finkel, R.C., McAninch, J., 2007. Absolute calibration of ^{10}Be AMS standards. Nucl. Instrum. Meth. Phys. Res. B 258, 403–413.
Ó Cofaigh, C., Dowdeswell, J., Jennings, A., Hogan, K., Kilfeather, A., Hiemstra, J., Noormets, R., Evans, J., McCarthy, D., Andrews, J., 2013. An extensive and dynamic ice sheet on the West Greenland shelf during the last glacial cycle. Geology 41, 219–222.
Perren, B.B., Wolfe, A.P., Cooke, C.A., Kjær, K.H., Mazzucchi, D., Steig, E.J., 2012. Twentieth-century warming revives the world's northernmost lake. Geology 40, 1003–1006.
Quillmann, U., Andrews, J.T., Jennings, A.E., 2009. Radiocarbon Dates from Marine Sediment Cores of the Iceland, Greenland, and Northeast Canadian Arctic Shelves and Nares Strait. Institute of Arctic and Alpine Research Occasional Paper 59, pp. 14–15.
Rasch, M., 2000. Holocene relative sea level changes in Disko Bugt, West Greenland. J. Coast. Res. 16, 306–315.
Rignot, E., Kanagaratnam, P., 2006. Changes in the velocity structure of the Greenland Ice Sheet. Science 311, 986–990.
Rignot, E., Velicogna, I., van den Broeke, M.R., Monaghan, A., Lenaerts, J.T.M., 2011. Acceleration of the contribution of the Greenland and Antarctic ice sheets to sea level rise. Geophys. Res. Lett. 38, L05503.
Roberts, D.H., Long, A.J., 2005. Streamlined bedrock terrain and fast ice flow, Jakobshavns Isbrae, West Greenland: implications for ice stream and ice sheet dynamics. Boreas 34, 25–42.
Roberts, D.H., Rea, B.R., Lane, T.P., Schnabel, C., Rodés, A., 2013. New constraints on Greenland ice sheet dynamics during the last glacial cycle: evidence from the Uummannaq ice stream system. J. Geophys. Res. Earth Surf.
Rood, D.H., Hall, S., Guilderson, T.P., Finkel, R.C., Brown, T.A., 2010. Challenges and opportunities in high-precision Be-10 measurements at CAMS. Nucl. Instrum. Meth. Phys. Res. Sec. B Beam Interact. Mater. Atoms 268, 730–732.
Scambos, T.A., Bohlander, J., Shuman, C., Skvarca, P., 2004. Glacier acceleration and thinning after ice shelf collapse in the Larsen B embayment, Antarctica. Geophys. Res. Lett. 31, L18402.
Serreze, M.C., Barrett, A.P., Stroeve, J.C., Kindig, D.N., Holland, M.M., 2009. The emergence of surface-based Arctic amplification. Cryosphere 3, 11–19.
Stone, J.O., 2000. Air pressure and cosmogenic isotope production. J. Geophys. Res. 105, 23753–23759.
Vinther, B.M., Buchardt, S.L., Clausen, H.B., Dahl-Jensen, D., Johnsen, S.J., Fisher, D.A., Koerner, R.M., Raynaud, D., Lipenkov, V., Andersen, K.K., Blunier, T., Rasmussen, S.O., Steffensen, J.P., Svensson, A.M., 2009. Holocene thinning of the Greenland ice sheet. Nature 461, 385–388.
Weidick, A., 1968. Observations on some Holocene glacier fluctuations in west Greenland. Medd. Grønl. 165, 202.
Weidick, A., 1972. Rapport Grønlands Geologiske Undersøgelse. ^{14}C Dating of Survey Material Performed in 1971, vol. 41, pp. 1–39.
Weidick, A., 1974. Rapport Grønlands Geologiske Undersøgelse. ^{14}C Dating of Survey Material Performed in 1973, vol. 66, pp. 42–44.
Weidick, A., 1975. A Review of Quaternary Investigations in Greenland, vol. 70, p. 22.
Weidick, A., 1994. Rapport Grønlands Geologiske Undersølgelse. Historical Fluctuations of Calving Glaciers in South and West Greenland, vol. 161, pp. 73–79.
Weidick, A., Kelly, M., Bennike, O.L.E., 2004. Late Quaternary development of the southern sector of the Greenland Ice Sheet, with particular reference to the Qassimiut lobe. Boreas 33, 284–299.
Weidick, A., Oerter, H., Reeh, N., Thomsen, H.H., Thorning, L., 1990. The recession of the Inland Ice margin during the Holocene climatic optimum in the Jakobshavn Isfjord area of West Greenland. Global Planet. Change 2, 389–399.
Weidick, A., Bennike, O., 2007. Quaternary Glaciation History and Glaciology of Jakobshavn Isbræ and the Disko Bugt Region, West Greenland: a Review. Geological Survey of Denmark and Greenland.
Young, N.E., Briner, J.P., Axford, Y., Csatho, B., Babonis, G.S., Rood, D.H., Finkel, R.C., 2011a. Response of a marine-terminating Greenland outlet glacier to abrupt cooling 8200 and 9300 years ago. Geophys. Res. Lett. 38, L24701.
Young, N.E., Briner, J.P., Stewart, H.A., Axford, Y., Csatho, B., Rood, D.H., Finkel, R.C., 2011b. Response of Jakobshavn Isbræ, Greenland, to Holocene climate change. Geology 39, 131–134.
Young, N.E., Briner, J.P., Rood, D.H., Finkel, R.C., Corbett, L.B., Bierman, P.R., 2013a. Age of the Fjord Stade moraines in the Disko Bugt region, western Greenland, and the 9.3 and 8.2 ka cooling events. Quat. Sci. Rev. 60, 76–90.
Young, N.E., Schaefer, J.M., Briner, J.P., Goehring, B.M., 2013b. A precise ^{10}Be production-rate calibration for the Arctic. J. Quat. Sci. 28, 515–526.